

REPORT ON THE INTERNATIONAL HYPERSONICS  
CONFERENCE HELD BY THE AMERICAN ROCKET SOCIETY  
AT THE MASSACHUSETTS INSTITUTE OF TECHNOLOGY  
DURING AUGUST 16 - 18, 1961.

by  
G. R. Salter

Technical Note H4

Hypersonic Propulsion Research Laboratories

Department of Mechanical Engineering

McGill University

Montreal

August 1961

INTRODUCTION

1.0 This report briefly summarizes the papers read at the International Hypersonics Conference held by the American Rocket Society at M.I.T. during August 16 - 18, 1961.

A list of the papers and authors is given, and the preprints obtained are indicated. Those preprints not obtained have been applied for, and will be available in the near future.

2.0 List of Papers

<u>Number</u>	<u>Title</u>	<u>Author</u>	<u>Preprint</u>
1965-61	Leading Edge Problem at Hypersonic Speeds	Hakuro Oguchi	No
1966-61	Second-Order Boundary Layer Theory for Blunt Bodies in Hypersonic Flow	M. Van Dyke	Yes
1967-61	Rarefied Hypersonic Flow Over a Sphere	Levinsky and Yoshihara	Yes
1968-61	The Rayleigh Problem for a Dissociated Gas	Moore and Rae	Yes
1969-61	Aerodynamic Testing at Mach Numbers from 15 to 20	Lukasiewicz, Whitfield and Jackson	Yes
1970-61	The Duration and Properties of the Flow in a Hypersonic Shock Tunnel	Holder and Schultz	Yes
1971-61	An Evaluation of the Hypersonic Gun Tunnel	Bray	Yes
1972-61	Diagnostic Studies of a Low-Density Arc-Heated Wind Tunnel Stream	Talbot and Sherman	No
1973-61	Initial Results from a Low-Density, Hypervelocity Wind Tunnel	Potter, Kinslow, Arney and Bailey	Yes
1974-61	Chemical Kinetics: A General Introduction	Bauer	Yes
1975-61	Chemical Kinetics of High Temperature Air	Wray	Yes

<u>Number</u>	<u>Title</u>	<u>Author</u>	<u>Preprint</u>
1976-61	Chemical Effects in External Hypersonic Flows	Vaglio-Laurin and Bloom	Yes
1977-61	Flow of a Reacting Gas	Langelo	No
1978-61	Radiation at Hypersonic Speeds	Treanor	Yes
1979-61	Radiation from Non-Equilibrium Shock Front	Teare, Georgiev and Allen	No
1980-61	Slender Wings at High Angles of Attack in Hypersonic Flow	Cole and Brainerd	Yes
1981-61	On the Newtonian Theory of Hypersonic Flow at Large Distances from Bluff Axially Symetric Bodies	Freeman	Yes
1982-61	Shock Layer Structure and Entropy Layers in Hypersonic Conical Flows	Melnik and Scheuing	No
1983-61	A Theory of Entropy Layers and Nose Bluntress in Hypersonic Flow	Yakura	Yes
1984-61	The Free Flight Range: A Tool for Research in the Physics of High-Speed Flight	Charters	Yes
1985-61	A Survey of Shock Tube Research Related to the Aerophysics Problem of Hypersonic Flight	Lin	Yes
1986-61	Air Arc Simulation of Hypersonic Environments	Warren and Diaconis	No
1987-61	The Development of the Shock Tunnel and its Application to Hypersonic Flight	Hertzberg, Wittliff and Hall	No

### 3.0 Summaries of Papers

#### 3.1 Leading Edge Problem at Hypersonic Speeds

Due to lateness of arrival at the Conference and the fact that the preprint is not yet available, there is no information at the present time.

### 3.2 Second-Order Boundary Layer Theory for Blunt Bodies in Hypersonic Flow

Viscous hypersonic flow near the nose of a blunt body, such as a sphere, was considered on the basis of continuum theory. The gas was assumed to be perfect with constant specific heats and constant Prandtl numbers. The viscosity was assumed to vary as  $T^\omega$ .

It was pointed out that the "unrealistic" Newtonian limit, i.e. the case where  $\gamma \rightarrow 1$  as  $M_\infty \rightarrow \infty$  was excluded.

It was then possible to write

$$T_0/T \propto M_\infty^2 \quad \text{as } M \rightarrow \infty$$

The thickness of the full shock layer, the detached shock wave and the boundary layer were expressed as functions of free stream Mach number, Reynolds number and nose radius. There resulted in the formulation of a viscous hypersonic similarity parameter,  $\mathcal{E}$ , for blunt bodies in the hypersonic limit.

Discussion of the relative thickness of the boundary layer and shock wave lead to the conclusion that the "viscous layer regime" proposed by Hayes and Probstein can never exist.

Using individual velocity components rather than stream functions, the second-order boundary-layer theory was developed in a general form.

The analysis used the technique of inner (boundary layer) and outer (outside the boundary layer) expansions, the reason for the separate analysis being that the outer expansion fails within a distance of the order of  $(\mathcal{E}a)$  from the surface. ( $a$  = nose radius).

The second approximation was analyzed in detail, the following second-order effects being discussed: longitudinal curvature, transverse curvature, slip, temperature jump, entropy gradient, total enthalpy gradient and displacement.

The evaluation of these effects was outlined for a blunt body.

### 3.3 Rarefied Hypersonic Flow Over a Sphere

Attention was focused on the transition of the flow over a sphere from the high density case to the case in which the density was lowered to the extent that the shock wave and boundary layer merged.

The reason for the merging is that as free stream density decreases, at a constant  $M_\infty$ , the thickness of both the shock wave and boundary layer will increase. In general the shock wave thickness increases more rapidly than the boundary layer, and the inviscid region of separation reduces in thickness.

The shock wave and boundary layer are said to be "fully merged" when, due to further reductions in free stream density, the inviscid layer is entirely eliminated.

As to the validity of the Navier-Stokes equations within the shock structure, where macroscopic quantities such as temperature, vary appreciably over a mean free path, the authors mentioned that there is evidence (see preprint for references) that excellent agreement has been achieved between theory and experiment on normal shock structures.

A monatomic gas with a "billiard ball" model for the interaction potential was considered. In this way the coefficients of viscosity and heat conductivity were proportioned to  $\sqrt{T}$ .

To simplify the energy equation, the Prandtl number was taken as  $3/4$ .

Computations were carried out on an I.B.M. 704 digital computer for a constant free stream Mach number of 10. The Reynolds numbers considered, based on adiabatic stagnation temperature and density were  $10^4$ ,  $10^3$  and  $10^2$ . For these conditions, two cases were analyzed, namely the adiabatic wall condition and the cold wall condition. A monatomic gas with  $\gamma = 5/3$  was assumed throughout.

### 3.4 The Rayleigh Problem for a Dissociated Gas

Assuming a partially dissociated diatomic gas, initially at rest and in equilibrium, bounded by a surface at the same temperature as the gas, the cases of surface temperature jump and impulsive plate motion were treated.

The surface was assumed to have some given degree of catalytic efficiency for recombination.

The actions considered, i.e. sudden surface temperature drop and impulsive surface motion, are similar in that they both produce chemical non-equilibrium in a boundary layer, which grows with time outward from the surface. In the latter case the driving temperature change results from aerodynamic heating in the boundary layer.

The analysis of the problem was particularly interesting because of its comparative simplicity. The simplifying assumption, which allowed complete linearizations of the problems, was that the equilibrium increase of energy in dissociation was much greater

than that in the internal degrees of freedom, for a given temperature increase at constant pressure. In addition, the Prandtl and Lewis numbers were taken to be unity, thermal diffusion was neglected, and the boundary layer assumption of constant pressure was made.

The concept of "frozen heat blockage" was discussed for the surface temperature jump case. The blockage is caused by the fact that the atom concentration takes a finite time to adjust chemically to the lowered surface temperature. During the period of adjustment, the transport of the chemical component of enthalpy is retarded.

In discussing the case of sudden surface motion, it was pointed out that there would be no heat blockage because the enthalpy potential for the boundary layer would remain constant for both early and late times. At intermediate times, however, non-equilibrium effects cause the heat transfer coefficient to suffer a dip.

Due to the fact that both cases under consideration reach equilibrium by the same law, the late-time solution for the case of a combined temperature-velocity disturbance at the surface is independent of the particular combination of disturbances.

### 3.5 Aerodynamic Testing at Mach Numbers from 15 to 20.

This paper dealt with the development of electric-arc-heated, Hotshot, hypervelocity wind tunnels at the von Karman Gas Dynamics Facility of the Arnold Engineering Development Centre.

Gaseous and solid particle contamination were the early causes of serious errors in aerodynamic measurements, especially heat transfer rates. Gaseous contamination, which was due to oxygen depletion

caused by chamber and throat component oxidation, and hydrogen addition from the decomposition of nylon liners and insulators, was reduced by using nitrogen as the working gas and by replacing the nylon liners with metal.

The particle contamination problem was greatly overcome by a redesign to a coaxial electrode configuration and by the inclusion of a baffle plate.

Three measurements were taken in order to determine the progress being made in overcoming the problem of solid particle contamination.

These were:

1. Loss of electrode weight.
2. Increase in the weight of a collector located in the test section.
3. Stagnation point heat transfer rates on models with hemispherical noses.

These measurements were most sensitive to particle contamination, and comparison between the experimental and theoretical results indicated the degree of contamination.

The theoretical analyses were based on the Fay-Riddell theory, using a Lewis number of unity.

Two tunnels, Hotshot 1 and Hotshot 2, were discussed. Except for size and energy storage systems, the tunnels were similar.

Hotshot 1 has a 16 inch diameter test section. Electrical energy is stored in condenser banks. The arc is initiated by disintegrating a trigger wire with energy from a separate trigger condenser.



Hotshot 2 has a 50 inch diameter test section. Electrical energy is stored in an inductance coil and then transferred to the arc chamber.

Mach numbers in the region of 18 for Hotshot 1 and 18 to 22 for Hotshot 2 were achieved.

Other details of these tunnels may be obtained from the preprint.

After discussion of the tunnels, attention was given to drag data measured in four tunnels. The tunnels employed were the Hotshots 1 and 2, a low density, arc-heated nitrogen continuous tunnel ( $M = 9$ ) and a continuous Mach 8 tunnel using air.

It was shown that drag estimates based on simple theory for slender delta wing models result in over-estimates for both the hot and cold wall cases. Application of the same theory to the low-density data also resulted in an overestimate.

Shock shapes over slender blunt cones were shown to have slopes as predicted from theory; however, theoretical differences in shock shapes because of different nose geometries were not found.

Theoretically predicted over-expansion and pressure overshoot along the conical surfaces of slender blunted cones at hypersonic speeds were observed experimentally.

### 3.6 The Duration and Properties of the Flow in a Hypersonic Shock Tunnel.

After briefly mentioning the hypersonic and low-density facilities of the National Physical Laboratory, Teddington, England, the authors dealt with the wave formations and interactions occurring in shock tunnels.

One of the N.P.L. tunnels is fitted with an optional by-pass so that it may be used for either "straight-through" or for "reflected-shock" operation. Dimensions of this tunnel are as follows:

Driving and driven tube	6 inches dia.
Total length of tube	57.5 ft.
High pressure chamber length	6 ft. or 18.5 ft.
Nozzle - conical	Exit dia. 16 in. or 30 in.

The gases used are hydrogen, compressed to 1000 atmospheres, driving air. The maximum driving pressure in the 18.5 ft. section is limited to 750 atmospheres, but the 6 ft. section is stressed to 1000 atmospheres.

The mechanisms of reflection from the contact surface, reflected shock boundary-layer interaction and expansion wave from the diaphragm were discussed in some detail.

It is of interest to note that the sodium line reversal method is being used for temperature determination at the N.P.L. At present, the backing source has a maximum temperature of 3000 °K and cannot be used for Mach numbers greater than 5.5. Carbon-arcs or water-stabilized arcs will be used to extend the useful range.

The differences in the wave patterns between three Mach numbers -- one below tailoring, one tailored and one above, were clearly shown by pressure traces behind the reflected shock.

Four schlieren photographs at times 30, 82, 145 and 620 micro-seconds (after primary shock passed leading edge) of the flow over a flat plate at a Mach number of approximately 7.8, very clearly showed the

decrease in boundary layer depth as the Reynolds number increased upon arrival of a strong upstream-facing expansion wave formed in the nozzle.

It was concluded that sufficiently long running times can be achieved in shock tunnels if the tunnels are suitably designed.

### 3.7 An Evaluation of the Hypersonic Gun Tunnel.

This paper was divided into four sections:

1. The development of the hypersonic gun tunnel from other types of free piston compressor.
2. Description of the gun tunnel at Southampton University and experiments carried out to study its performance.
3. Comparison with other hypersonic facilities.
4. Aerodynamic testing in gun tunnels.

In the first section, a comparison was made between isentropic and shock wave compression, which immediately eliminated the former for hypersonic tunnel work on the grounds of overall dimensions and piston weight.

In order to achieve efficient conversion of the work done on the compressor into thermal energy in the test gas, a low mass (high velocity) piston is required.

Ideal gas and real gas performance estimates, which indicated that very high stagnation temperatures and long running times of the order of tenths of seconds could be achieved, were not realized in practice because of piston failure. It was stated that an order of magnitude improvement in piston strength is required before the very high

stagnation temperatures envisaged could be reached. It was also found that the large rate of fall of stagnation temperature severely curtailed the useful running time, although a flow duration greater than that normally produced in a conventional shock tunnel could easily be obtained.

The author emphasized the point that the longer running times are particularly useful in certain aerodynamic tests. Amongst those mentioned were the testing of hypersonic air intakes, separated hypersonic flows, and force and moment measurements on models.

It was shown that the high peak pressure due to piston overshoot could be entirely eliminated if a sufficiently light piston were used, and it was concluded that any reflected shock tunnel might be used in the manner of a gun tunnel for tests requiring an extended running time at comparatively modest stagnation temperatures.

### 3.8 Diagnostic Studies of a Low-Density Arc-Heated Wind Tunnel Stream.

The University of California arc-heated argon tunnel was described.

The operating conditions, which were achieved with an input of 12 K-W were as follows:

1. Stagnation temperature	5000 to 9000 °K
2. Mach number	4.5 to 13
3. Pressure	1/2 atmosphere
4. Reynolds number per cm or behind the shock	200 to 650 10 to 100
5. Mean free path	1/100 to 1/10 cm
6. Ionization	.3 to .4%

The hypersonic nozzle, which had a copper throat, had an initial 8 1/2 degree conical expansion followed by a 13 1/2 degree expansion. A coil of a few hundred gauss, taking a current of 1/2 to 1 amp, was used to pinch the stream around the anode.

A point of practical interest was that boron nitride was used for insulation in the heat transfer probes.

The experimental results showed that:

1. The axial pressure distribution was smooth, showing that there were no oblique shocks present.
2. There was no overlapping of the boundary layer in the radial distributions.

### 3.9 Initial Results from a Low-Density, Hypervelocity Wind Tunnel.

The L.D.H. (low-density hypersonic) tunnel described in this paper was a continuous arc-heated type, usually using nitrogen as the working fluid.

The arc-heater normally operated at less than 20 KW.

The tunnel Mach number of 9 to 11 combined with the Unit Reynolds number of 220 to 420 per inch represented speed (7000 to 10,000 ft/sec) and density conditions of high speed flight at an altitude of 50 miles.

The hypersonic nozzle exit diameter of 5.84 inches was reduced by boundary layer thickness to a useful core of uniform flow of approximately 1 inch in diameter. This situation was achieved with a favourable boundary layer temperature gradient,  $T_w/T_o \approx 1/10$ , obtained by water cooling the tunnel walls.

Most of the paper was devoted to a discussion of the probes developed and used in the subsequent testing.

Flat-faced, water-cooled, impact pressure probes were used, and it was concluded that little more than 2% error in impact pressure existed. It was found that corrections for the temperature gradient along the probe did not produce a significant change in the results. Exploratory measurements were made with a family of static pressure probes having conical noses and cylindrical afterbodies. The orifice locations were at varying distances from the stagnation points. It was hoped that the free stream static pressure could be determined by extrapolation of the pressure distribution along the probe to the limit of infinite length. It was felt that the results were reasonably promising, but that detailed discussion was not justified at the present time because of the effects of nozzle axial pressure gradient and thermal gradient along the probe.

Very encouraging preliminary results were obtained from a mass-flow probe. The method was to measure the displacement of oil over a measured period of time. The most crucial factor in the procedure was the swallowing of the shock wave at probe inlet. Further research is being conducted on this method of measurement.

Although not usually incorporated in low-density tunnels, a diffuser was found to give an improvement in nozzle pressure ratio. Diffusers of different dimensions were tested.

A limited series of drag measurements were completed on solid steel spheres. Correlation of the data with that from other sources was

possible on the basis of the parameter  $(C_D - C_{D_c}) / (C_{D_{fm}} - C_{D_c})$  being plotted against Reynolds number. Here  $C_D$  was the measured drag co-efficient,  $C_{D_c}$  was that at high Reynolds number, and  $C_{D_{fm}}$  was that for free-molecular flow. In this way the variations in  $C_D$  due to differences in Mach number, temperatures and heat transfer tended to vanish.

### 3.10 Chemical Kinetics: A General Introduction.

The paper began with an outline of the postulates of chemical kinetics, and it was pointed out early in the discussion that the assumption that rate constants are functions of temperature only is not valid under conditions where the rates involved affect the Boltzmann distribution for the system.

The author raised the question as to how one determines the mechanisms of complex reactions. Experimental determination of the parameters occurring in the "mass action law" for the particular reaction was the first step. Then the use of spectroscopic or chemical methods, the injection of intermediates by photochemical means, the use of isotropic tracers, or one of many other techniques could be used to detect the presence of suspected intermediates.

It was emphasized that for each step in a reaction one may write an equilibrium constant as a ratio of forward-to-reverse rate constants; but that one could not state that, in a system for which the mechanism was not known, the over-all equilibrium constant was equal to the ratio of rate constants which specified the rates of appearance and disappearance of a selected reactant under arbitrary conditions.

For flow systems in which steady state had been achieved, and in which the lag in the chemical process behind gas dynamic changes was small, it was shown that introduction of the so called "affinity function" would serve to linearize the rate equations so that near to equilibrium all reactions would be pseudo-first order and a relaxation time could be defined.

On the subject of molecular theories for the determination of reaction rate constants, Dr. Bauer gave the following reasons for the disappointing results to date:

1. Molecular collisions are complex processes in themselves, and additional complications are introduced by quantum limitations when energy and momentum are transferred.
2. Contributions from the different energy modes are not predictable because the effectiveness of coupling between the internal degrees of freedom depends sensitively on the details of the collision.
3. The quantum mechanical transition probability for a specified reaction path and relative energy requires the introduction of semi-empirical relationships for all but the simplest systems.
4. The distinction between highly excited reactants and products is inherently vague.

Attention was then focused on gas dynamics plus chemical kinetics. The line reversal technique, using a small amount of  $C_r(CO)_6$  as a tracer element, was found to be the most reliable means of measuring shock temperatures. It was noted that the reading should be made 30 to 50 micro-seconds after passage of the shock to allow for relaxation effects.



Discussions concerning the dissociation of diatomic and polyatomic molecules, reaction rates in nozzles, and isotope exchange reactions completed the paper.

### 3.11 Chemical Kinetics of High Temperature Air.

Air was considered as a simple oxygen-nitrogen mixture. The temperature range taken was 3000 to 8000 °K. The significant reactions occurring were listed, and equations of the form  $K = AT^n \exp (-D/RT)$  were fitted for each of the equilibrium constants.

Vibrational relaxation times and dissociation rates for oxygen, nitrogen and nitric oxide were taken from various sources.

Similarly, data on the nitric oxide reactions,



were summarized and discussed.

The large overshoot in NO concentration during the relaxation period, caused by the rapidity of the last two equations above, was mentioned.

The ionization reaction,  $\text{N} + \text{O} + 2.8 \text{ ev} \rightleftharpoons \text{NO}^+ + \text{e}$ , was mentioned briefly.

Time histories from the shock front to full equilibrium were computed for three shock speeds in air. The dominant reactions for each case were discussed.

### 3.12 Chemical Effects in External Hypersonic Flows.

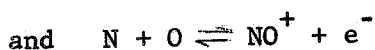
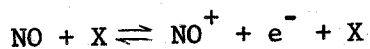
The flow field surrounding a blunt-nosed slender body at zero angle of attack was divided into regions of inviscid and viscous flow.

Analysis of the inviscid flow showed that the use of a simplified model in conjunction with one-dimensional rate calculations along streamlines lead to reasonably accurate descriptions of the actual situation. The simplified approach assumed that across strong portions of a shock the gas is chemically frozen near sonic velocity, while the gas crossing weaker portions is frozen at post-shock equilibrium conditions.

To study the flow in the entropy layer close to the nose, the region was divided into two layers by a streamline inclined at approximately  $20^\circ$  to the shock for satellite velocities. The inner layer was characterized by constant pressure and the outer layer by a self-similar small perturbation solution.

Analysis of regions of viscous flows emphasized both laminar and turbulent wakes.

Non-equilibrium effects, as far as the ionization reactions



were concerned, in consideration of the inviscid flow and wake showed the necessity of performing rate calculations case by case.

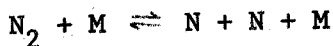
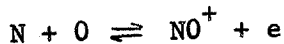
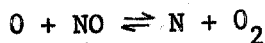
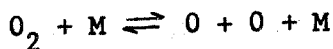
It was also shown that departures from equilibrium in the boundary layer on a non-catalytic cold wall followed a history that was quite different from that of the inviscid flow.

### 3.13 Flow of a Reacting Gas.

Calculations of temperature ratios and electron densities as functions of distances along stream lines were made for  $90^\circ$ ,  $60^\circ$  and  $30^\circ$  shocks. The velocities used were 20,000, 30,000, and 40,000 ft/sec, and the altitudes considered were 300,000 ft. and 250,000 ft.

Diffusion, heat transmission and viscous effects were neglected and it was assumed that the translational, rotational and vibrational modes were in equilibrium.

The air model chosen was assumed to obey the following reactions:



The temperature ratio curves followed the trend expected in that the values for the 30,000 ft/sec. case lay between those of the higher and lower velocity cases.

An unexplained discrepancy arose, however, in the curves of electron density, where the 40,000 ft/sec case fell between the 20,000 and 30,000 ft/sec values.

The flow along chosen streamlines between a blunt nosed  $30^\circ$  cone and the shock, at  $M_\infty = 20$  and altitude = 200,000 ft, were computed. The results were plotted as temperature and electron density for equilibrium and non-equilibrium flows.

### 3.14 Radiation at Hypersonic Speeds.

Optical radiation from the heated air surrounding a hypersonic body serves as a means of observation of re-entering vehicles. This, together with the radiative contribution to heat transfer, has initiated extensive research in this field.

The author of the paper enumerated the problem as the determination of:

1. The number density of the chemical species present in the flow.
2. The degree of optical excitation of the species.
3. The radiation that would be obtained from each species for a specified degree of excitation.

These problems were discussed, and data was compiled from various sources.

Radiation measurements for molecules of oxygen, nitrogen, nitric oxide and nitrogen dioxide, and free electron radiation were dealt with.

### 3.15 Radiation from Non-Equilibrium Shock Front.

Not attended.

### 3.16 Slender Wings at High Angles of Attack in Hypersonic Flow

From an integrated strip approach, surface pressure and velocity distributions were calculated from Newtonian theory. Boundary layer theory was then applied to give the external conditions. For this method to be effective, the flow over the surface must be essentially two-dimensional. This difficulty was overcome by the introduction of an inner region, adjacent to the surface, in which the orders of magnitude of the various perturbations were

changed from those in the region near the shock. Matching of the inner and outer solutions enabled the complete flow field to be determined.

Shock detachment distance, shock wave shape and heat transfer distributions were calculated. Fairly good agreement with experimental data on delta wings at angles of attack near  $90^\circ$  was found.

### 3.17 On the Newtonian Theory of Hypersonic Flow at Large Distances from Bluff Axially Symetric Bodies

The object of this paper was to clarify the relationship between the "free layer" theory and the asymptotic solution to the "blast wave analogy". The body was assumed cylindrical with a hemispherical nose.

It was pointed out that if the two theories are correctly derived from the complete solution to the problem, then they may be regarded as different methods of expansion of this solution. The derivation of higher order terms in  $(\gamma - 1)$ , in consideration of the asymptotic behaviour of the free layer at large distances, showed that these quickly dominated the first order ones. It was therefore, necessary to seek a solution which was uniformly valid in the limit of large distances and  $\gamma \rightarrow 1$  and which would give a description of the flow field far from the body.

An expression for the shock wave shape was derived from which surface pressure could be calculated. The behaviour described resulted in a flow comprising a thin outer centrifugal layer close to the shock with a wide inner entropy layer.

Extensions of the theory to other body shapes were considered.

### 3.18 Shock Layer Structure and Entropy Layers in Hypersonic Conical Flows

The paper began with a review of the work done by Gonor, Cheng, Freeman and Guiraud on the hypersonic flow over yawed conical surfaces. None of the investigators but Cheng was concerned with the problem of obtaining a solution valid in the entire region of disturbance surrounding the body. Cheng's analysis was restricted to small deviations from axial symmetry.

It was shown that nonuniformities and the associated entropy layers occur in other more general cases, and the problem of obtaining uniformly valid solutions in the thin-shock-layer limit was the topic of the paper.

### 3.19 A Theory of Entropy Layers and Nose Bluntness in Hypersonic Flow

By applying the method of inner and outer expansions to the inverse problem, in which the body profile is determined for a given shock shape, uniformly valid solutions far downstream from the blunt nose of slender bodies were obtained for hyperbolic and power-law shock shapes.

An inviscid perfect gas and an infinite Mach number were assumed.

It was found that the flow field resulting from the body that produces a paraboloidal shock may be asymptotically represented by the solution for the analogous constant-energy explosion.

Similar results were obtained for the two-dimensional case of the  $2/3$  power-law shock.

### 3.20 The Free Flight Range

The accelerated-reservoir light-gas gun, developed by Curtis of the Ames Research Centre, was described. Hydrogen, compressed by a piston driven down a pump tube by a charge of gun powder, flows through the tapered bore of a high pressure coupling and accelerates a model down the launch tube. The face of the piston, being made of a plastic material, deforms in the high pressure coupling and so accelerates along the tapered bore. The design is such that the rising pressure caused by this acceleration counteracts the falling pressure on the base of the sabot.

A method of measuring stagnation point heat transfer was described. A thermocouple and coil in the head of the projectile create a magnetic field which is recorded by means of stationary pick-up coils. The results agree well with theory and with shock tube measurements.

In conclusion, it was suggested that the capabilities of the range could be extended by replacing the flight-test chamber with the working sections of supersonic, hypersonic, or shock-tube wind tunnels.

### 3.21 A Survey of Shock Tube Research Related to the Aerophysics Problem of Hypersonic Flight

This paper was a preliminary effort to compile published works pertaining to shock tubes. The preprint should prove to be a useful reference for most aspects of shock tube testing.

### 3.22 Air Arc Simulation of Hypersonic Environments

The basic object of the facilities described was to study the response of heat protection systems.

The lecture commenced with a discussion of the re-entry vehicle flight spectrum in terms of stagnation enthalpy, stagnation pressure and altitude. Both ablation, (short time, high heating rates) and re-radiation, (long time, high total heating) were of interest.

The types of arcs mentioned were:

- |                             |                                    |
|-----------------------------|------------------------------------|
| 1. Free arcs                | 2 electrode D.C., 3 electrode A.C. |
| 2. Vortex axial flow        | water arc D.C., gas D.C.           |
| 3. Magnetically driven arcs | D.C. and ring electrode A.C.       |
| 4. Divided flow             | D.C.                               |

In the divided flow type, the test plasma had little electrode contamination. The contaminated flow was removed through openings just above the electrodes.

The test configurations for arc facilities were classed as:

1. Subsonic free jet.
2. Supersonic free atmosphere jet.
3. Supersonic tunnel.
4. Shrouded nozzle.
5. Simple pipe model
6. Contoured pipe model.

The big advantage with the supersonic tunnel configuration was that it provided for pressure reduction around the model.



The advantage of the shrouded nozzle type was that for a given power, the largest model could be tested.

The arc levels considered were in the region of 10 mega-watts in the electrodes producing a stream enthalpy of 20,000 BTU/lb. Pressures in the region of 1500 psi have been reported, but at fairly low enthalpies ( $\approx 5,000$  BTU/lb).

Enthalpy measurements were made:

1. Calorimetrically;
2. Spectrascopically.

It was felt that the accuracy of the spectrascopic measurements, from which the electron temperature of the flow was determined, was  $\pm 5\%$ .

Since agreement was found in the electron and calorimetrically determined temperatures it was inferred that the flow was in equilibrium.

### 3.23 The Development of the Shock Tunnel and its Application to Hypersonic Flight

The limitations of the shock tunnel, i.e. that only one or two of the flow parameters could be duplicated in any test, were mentioned.

The need for a truly adequate driver was discussed, and this could be achieved in the following manner. Hydrogen, pre-heated to  $1000^{\circ}\text{C}$  would be further heated to  $2000^{\circ}\text{C}$  by means of a gun tunnel. This high temperature, high pressure gas would then be used as the driver for the shock tunnel.

Dr. Hertzberg thought that the problem of radiation loss was not serious, but that the non equilibrium flow problem demanded a great deal of attention.